PHYSICAL REVIEW B VOLUME 14, NUMBER 8 15 OCTOBER 1976

Energy-loss spectra of Mo(100) clean and covered with oxygen

Y. Ballu, J. Lecante, and H. Rousseau
Service de Physique Atomique, Section d'Etudes des Interactions Gaz-Solides, Centre d'Etudes Nucléaires de Saclay, Boite Postale No. 2, 91190 Gif-sur-Yvette, France
(Received 21 November 1974)

A high-resolution electron-impact spectrometer has been used to study the inelastic scattering of slow electrons (about 60 eV) on a molybdenum (100) face either clean or covered with oxygen. Surface effects were emphasized by the reflection technique on a massive sample. Energy-loss spectra are given which show features due to single and collective excitations of the conduction electrons. Volume and surface plasmons are identified, the latter by comparison with optical data and by its angular dependence. During oxygen adsorption the intensity and the position of the surface-plasmon peak are deeply modified and new peaks appear which are due to the excitation of molecular orbitals formed by chemisorption. These observations are related to the adsorption kinetics of oxygen on the (100) molybdenum face.

I. INTRODUCTION

In order to understand chemisorption mechanisms one needs a great deal of information coming from various experimental techniques. Thermal desorption has been for a long time the only way to obtain such information; in principle it can give the binding energy and coverage of the adsorbed species. Nevertheless there are many drawbacks in the interpretation of flash desorption measurements: the binding energies of adsorbed particles are very difficult to obtain and the results are always questionable on experimental and theoretical grounds.

Other techniques such as low-energy-electron diffraction (LEED), and work-function measurements suffer from similar deficiencies in the interpretation of experimental results.

The recent advances in spectroscopic techniques seem to be very promising. A "surface spectroscopy" field is now growing and enables us to obtain information on the electronic structure of adsorbate-adsorbent systems. These techniques are generally identified by the "means" employed to extract electrons from the surface layer: photoemission,[1] field emission,[2] ion-neutralization spectroscopy (INS),[3] and energy-loss spectroscopy (ELS).[4] Information thus obtained is very valuable in understanding the nature of the surface bond. Nevertheless such information is often very difficult to extract from the primitive electron energy distribution. The local density of state is not easily attained, it needs important mathematical treatments (INS) and there are many spurious effects such as the inelastic collisions suffered by the ejected electron along its escape path. These inelastic effects are very pronounced at low energy and they strongly affect the results of low-energy-electron spectroscopy.

Thus at the present time "surface spectroscopy" techniques are only used to give qualitative and semiquantitative information on the local density of states of surfaces which are clean or covered with adsorbates. The results must always be compared with the results obtained by other "classical" methods, and it is only when all the available information is gathered that a more realistic model for the surface bond can be constructed.

The purpose of the present paper is to give the results we have obtained on the electronic properties of a (100) molybdenum surface by electron-energy-loss spectroscopy. We used the reflection of slow electrons (20 to 100 eV) on a thick sample. This method is very surface sensitive owing to the small penetration of the incident beam and the small escape depth of the ejected electrons (less than 5 Å for electron energies between 50 and 150 eV).

The characteristic energy-loss spectra are mainly constituted by peaks due to the excitation of collective oscillations (bulk and surface plasmons) and interband transitions. These spectra are complicated, but much information can be extracted from them by using a complete analysis method.

The adsorption of oxygen or residual gases has shown the existence of electronic levels of the metal very sensitive to the surface state. New levels appeared due to the adsorption of oxygen and an attempt was made to correlate these levels and the changes in elastic and inelastic intensities to the adsorption kinetics of oxygen.

II. EXPERIMENTAL TECHNIQUES

A. Specimen treatment

A single crystal of Mo [(100) face] was mounted in an ultrahigh-vacuum chamber which had an ultimate pressure in the 10^{-10}-Torr range (residu-

al components: 85% H_2 and 15% CO).

The crystal target, a 6-mm-diam disk, 0.2 mm thick, was spot-welded to a small tantalum ribbon fixed to the sample holder. Heating was obtained by bombarding the reverse side of the sample with a small electron gun attached to the holder. Temperature was measured by a W-W-Rh thermocouple spot-welded to the crystal. Surface cleaning was done *in situ* by alternate heating and oxidation. The cleaning procedure was determined in a similar apparatus using a three-grid LEED-Auger system; it consists of heating to 1400°K in 10^{-6} Torr of oxygen for a cumulative time of 10 h, and annealing by several flashes in high vacuum to 1800°K until the oxygen was removed from the surface.

After several cycles of such treatment the Auger spectra revealed no surface impurities.[5] In the electron spectrometer apparatus, the cleanliness of the surface was checked by work-function-change measurements during the adsorption of a given pure gas. This procedure was used because of the poor sensitivity of the Auger spectroscopy performed with the electron spectrometer in its present configuration. In the present version the scattering angle is fixed at 120°, which is not the best configuration to emphasize the Auger effect[6] and Auger spectroscopy needs a high primary energy which could not be obtained in our apparatus. The test gases were introduced into the chamber by a small capillary placed just in front of the target. The gas flux was determined by measuring the pressure drop between two points of the capillary. Thus during an adsorption cycle on the target surface, the pressure in the chamber near the electron spectrometer was maintained in the 10^{-10}-Torr range whereas the equivalent pressure in front of the target was in the 10^{-8}-Torr range. The small variation of the overall pressure thus prevents any change of the current delivered by the monochromator.

B. Electron spectrometer

The electron spectrometer consists of two 127° cylindrical condensers.[7] The first condenser is used as a monochromator for an electron beam issuing from a tungsten hairpin filament. The monochromatized beam is then scattered by the target and energy analyzed by the second condenser. The backscattered electrons after analysis are counted with a channel multiplier (Fig. 1 shows a schematic view of the electron spectrometer and counting system). Both condensers are fixed, the scattering angle being 120°. The target can be rotated around the vertical axis and moved along this axis. During the cleaning process the target was withdrawn from the measurement cell in order to avoid contamination of this cell by sputtered or evaporated particles. The entire apparatus, condensers and cell, is made of stainless steel and is surrounded by a double "conetic" shield which reduces the magnetic field to less than 0.01 G. The entrance lens of the analyzer (a 3-mm-diam hole) allowed only electrons emitted within a cone of 15° to enter the analyzer, the other lenses reducing the acceptance angle to the overall angular resolution less than ±1°. The primary energy used in these experiments was varied in the range 20–100 eV. The best resolution obtained with the whole system appeared to be 40 meV full width at half-maximum (FWHM) and is consistent with the theoretical limit.[8] For the energy-loss measurements this ultimate resolution was unnecessary and instead we maximized the target current. Typically, for 10^{-9} A of 60-eV incident electrons, the FWHM of the elastically reflected peak is 200 meV. For the energy analysis, the whole target and monochromator system is swept while the analyzer is maintained constant with respect to the ground. This means that we use a fixed pass energy and sweep the retarding field; therefore, the spectrum produces the actual energy distribution.

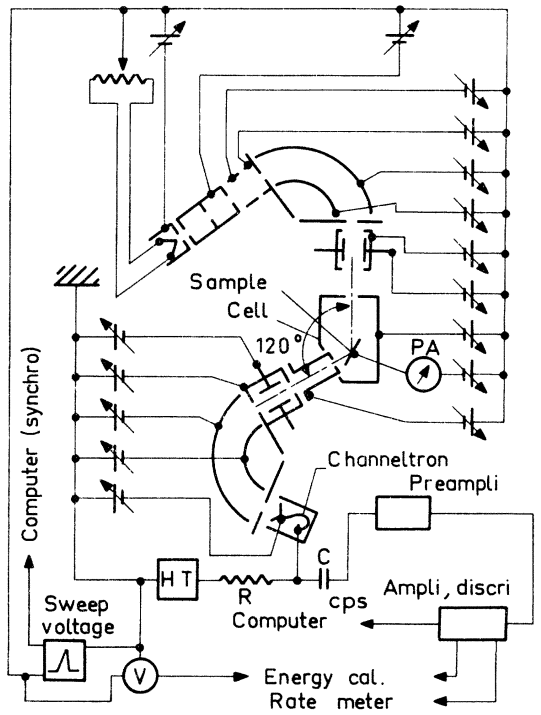

FIG. 1. Electron spectrometer and electric circuit. PA: picoammeter; HT: high tension.

C. Work-function measurements

Variations in the target surface potential were determined with the monochromatized beam. A retarding potential was applied to the crystal and the collected current was plotted on an XY recorder. The work-function changes were measured by the shift of the curves thus obtained. The advantage of using a monochromatized beam is twofold: first, the curves are steep and thus the accuracy is good, and second, the reference potential delivered by the monochromator is constant to the extent that the potential difference between the deflecting electrodes is constant.

III. RESULTS AND DISCUSSION

A. Curve analysis

Figure 2 shows the energy-distribution curves of electrons backscattered by a clean (100) molybdenum surface, the primary energy being varied from 50 to 80 eV. We have only represented an energy range extending over about 20 eV from the elastic peak. This part of the spectrum is mainly due to electrons that have suffered discrete energy losses on scattering. We can see that the various peaks vary little in energy loss ΔE but strongly in amplitude energy E_p. The spectra are complicated and very difficult to interpret but we can tentatively identify certain peaks. In order to determine the number of principal lines, their shape, and approximate intensity, we have used the following analytical method illustrated in Fig. 3(a):

(i) A continuous curve (dashed lines) obtained by adjusting a parabola to the background contribution is subtracted from the experimental points. This background may be due to electrons which have undergone multiple inelastic scattering and it acts so to shift the poorly resolved lines due to single-scattering events.

(ii) The number of peaks present in the spectrum is evaluated and the corresponding number of adjustable Lorentzian curves is fitted to the curve obtained in (i). After an optimization process the summation of the Lorentzian curves and the background contribution must give the initial experimental spectrum. If the fitting is not good it may appear that the number and assigned primitive position of the individual lines are not correct and the process is repeated with a different choice of

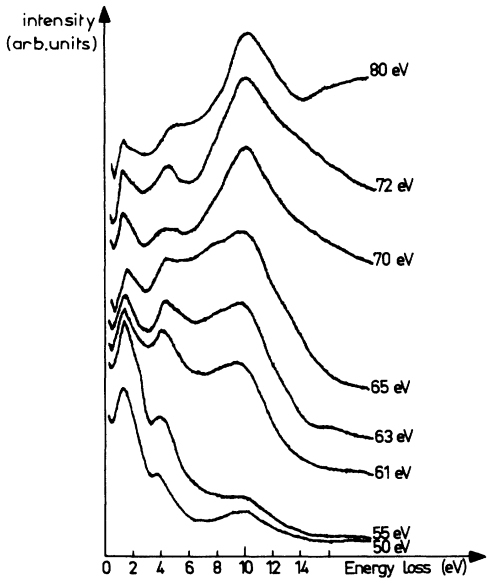

FIG. 2. Energy-distribution curves of electrons backscattered by the clean (100) molybdenum surface. The primary energy was varied from 50 to 80 eV.

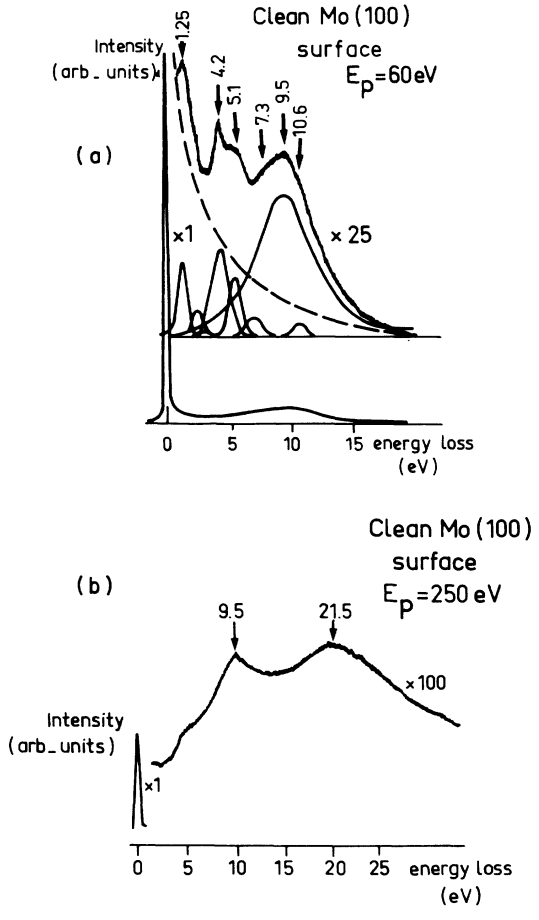

FIG. 3. (a) Curve analysis (clean surface, $E_p = 60$ eV). The dashed curve is the background contribution subtracted from the experimental points. (b) Energy-distribution curve for 250-eV primary energy showing the surface and volume plasmons.

parameter. The observation of various spectra, their modifications during adsorption processes for instance, greatly facilitate such a choice. All these operations are controlled by the scope of a display unit connected to a computer. Lorentzian profiles have been chosen because they fit fairly well the peaks observed during this study, but other profiles can be used.

B. Choice of the primary energy

Now, what is the best primary energy value for observing spectra with important structure and if possible where the surface effects are emphasized?

In the case of reflection on a massive sample two processes are required to reverse the direction of incident electrons[9] because the momentum transfer due to inelastic scattering alone is not sufficient for that and complementary elastic scattering by the lattice is needed. Thus we can expect great sensitivity on energy-loss spectra obtained at those primary energies where a diffraction condition is satisfied.

If we assume a two-step model for scattering,[10] i.e., kinematical elastic diffraction before the loss process, we must take for the primary energy, the energy corresponding to the classical Bragg peaks in the intensity distribution of the (00) beam.

We calculate these energies using the formula

$$V = \frac{150.4 n^2}{4a^2 \cos^2\psi} - \frac{V_i}{\cos^2\psi},$$

where V is the primary energy in eV giving a Bragg peak, a is the lattice parameter (3.14 Å for Mo), and ψ is the incidence angle with respect to the surface normal, in our case $\psi = 60°$, V_i is the inner potential; for instance, in the case of W(100) this potential is taken to be 15 eV for a beam normal to the surface.[11] But the value of V_i is different according to the diffracted beam or incident angle.[12] The experimental curve for the elastic intensity of the (00) beam versus the primary shows a peak near an energy of 60 eV.

If we use the formula with $V_i = 0$, we find

$$V = 60 \text{ eV}.$$

Thus, in our case, with an incident angle of 60° a Bragg condition may be satisfied for a primary energy of 60 eV.

For these conditions, if the two-step process is predominant, we have to choose a primary energy near 60 eV.

On the other hand, if we consider the curve giving the escape depth of electrons versus energy,[13] we find that there is a minimum for energies between 50 and 100 eV. In this energy range the surface effects will be enhanced relative to the bulk effects. In our case, where we analyze electrons which have lost only a small amount of energy we have to choose the primary energy in this range.

Thus we have been led to adopt a primary energy of 62 eV, which proves to give more significant and surface-sensitive structures.

C. Clean surface

Figure 3(a) shows the curve analysis of the energy distribution of 60-eV electrons backscattered by the clean (100) Mo surface. Table I lists the main losses observed, their FWHM, and their intensity relative to the elastic peak. The normalization of the loss peaks to the elastic peak intensity appeared to be necessary, particularly if we want to obtain measurements of the intensity of certain loss peaks during a change of the surface state. During the experiments the intensity of the incident beam is kept constant, but owing to the adsorption of foreign species, the intensity of the elastically reflected beam in the specular direction may be profoundly modified (surface barrier, new surface structures). It is an experimental fact that, in our geometry, the loss peak intensities roughly follow the variations of the elastic peak. This is not surprising if we consider that the electrons we analyze are probably first elastically scattered by the lattice and then suffer inelastic collisions with small momentum changes. This hypothesis is probably valid in our experiment, where we observe the electrons scattered in a small cone centered on the specular direction.

In Table I we have only reported the losses smaller than 15 eV. Other features are present above 15 eV, in particular a broad peak centered at about 21.5 eV becomes preponderant as the primary energy is increased [see Fig. 3(b), which gives a spectrum obtained at 250 eV].

TABLE I. Characteristic values for different peaks obtained at a 70-eV primary energy.

Peak location (eV)	2.4	3.1	4.2	5.1	7.0	9.5	10.6
FWHM (eV)	0.8	0.6	1.2	1.4	1.7	5.3	0.9
Intensity relative to elastic peak intensity	0.002	0.001	0.011	0.007	0.002	0.017	0.002

1. Plasmon lines

Among the structures observed in the characteristic losses, those at 9.5 and 21.5 eV may be attributed to the excitation of, respectively, the surface and volume plasmons. Although Mo is not a free-electron metal we observe that the 21.5-eV lens corresponds roughly to the collective oscillations of the six valence electrons of Mo($4d^5$, $5s^1$).

The well known formula

$$\omega_p = (4\pi ne^2/m)^{1/2}$$

applied to the case of molybdenum (with $n = 6$ electrons per atom) gives a "free-electron" plasma frequency of $\omega_p = 3.5\times 10^{16}$ sec^{-1}, corresponding to an energy $\omega_p = 23$ eV. Lynch and Swan[14] reported for polycrystalline Mo an energy loss of 22.8 eV and attributed it to the volume-plasmon excitation. In a LEED apparatus we have also observed for the (100) face of Mo an energy loss centered at 23 eV.[15] It seems that the plasmon energy obtained in retarding-potential measurements integrated over a wide range of scattering angle is higher and approaches the theoretical value. This fact may be interpreted as due to a dispersion effect. We know that the plasma frequency presents a dispersion relation[16] $\omega(K)$:

$$\omega_p = \omega_{p0}\left(1 + \frac{3}{10}\,\frac{V_F^2 K^2}{\omega_0^2} + \cdots\right),$$

where K is the wave vector of the plasma oscillations and ω_{p0} the value of the plasma frequency for small values of K. Thus we can see in the simplest case of transmission through a thin film that the smaller losses due to plasmons are measured for a scattering angle equal to zero whereas greater values are given for a finite scattering angle: $K = K_{el}\theta$, where K_{el} and K are, respectively, the incident electron and plasmon momentum, and θ is the scattering angle[16] (see Fig. 4).

The same argument must apply in reflection experiments around the specularly reflected beam, thus explaining the greater values given by experiments which integrate the reflected current over a wide solid angle. We have attributed the 9.5-eV loss to the excitation of surface plasmons, though the free-electron value given by the formula $\hbar\omega_s = \hbar\omega_p/\sqrt{2}$ is 16 eV,[17] and we do not find any peak in this energy range for the clean surface. That the molybdenum does not act as a free-electron metal is not surprising and the plasma frequencies may be shifted by low- or high-lying interband transitions. Thus for molybdenum as for tungsten the volume plasma frequency is coincident with the free-electron value.

Other reasons strengthen the idea of plasma oscillations for the 9.5 and 21.5 losses:

(i) The variations of the relative intensities of these peaks when the incident beam voltage is modified: the 9.5-to-21.5-eV-loss intensity ratio decreases when the primary energy increases from 100 to 150 eV.

(ii) The 9.5-ev loss is very sensitive to the surface cleanliness; we shall discuss this in Sec. IV.

(iii) The comparison with available optical data. For a metal bounded by vacuum the excitation probability for the surface plasmon is proportional to the function $-\mathrm{Im}[1+\epsilon(\omega)]^{-1}$, where $\epsilon(\omega) = \epsilon_1(\omega) + i\epsilon_2(\omega)$ is the complex dielectric constant of the free-electron gas. Using the values of ϵ_1 and ϵ_2 given by reflectance measurements[18] we can plot the curve $-\mathrm{Im}[1+\epsilon(\omega)]^{-1}$ versus ω. This curve has a maximum near the energy $\simeq$10 eV, which is in good agreement with the experimental value of 9.5 eV.

(iv) The angular dependence of the intensity of the surface-plasmon peak. In the present apparatus, the scattering angle is fixed but we may rotate the target so that we can measure the relative intensity of the 9.5-eV peak for different combinations of incidence and emergence angles. The target was rotated on both sides around the specular position and the absolute intensities of elastic and 9.5-eV peaks were measured for various angles. Figure 5 shows the results, the angle γ, being

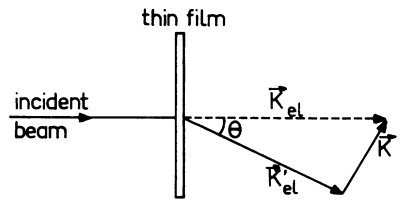

FIG. 4. Momentum change of an electron passing through a thin film.

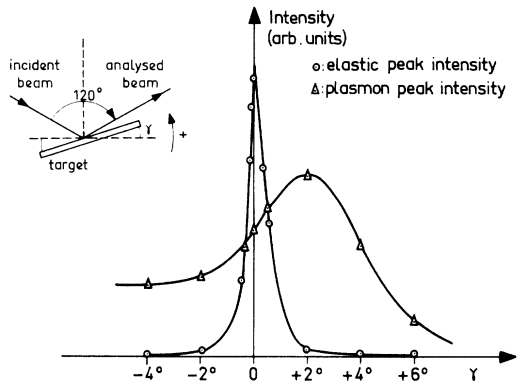

FIG. 5. Effects on elastic and plasmon peak of the target rotation.

measured from the specular position, a positive angle corresponding to an incident beam closer to the surface normal, or a more grazing emergence. We can see that whereas the elastic peak is symmetrical with respect to the rotation, the loss peak is not symmetrical and presents a maximum in a direction different from the specular reflection. Other peaks, e.g., due to interband transitions, have a behavior similar to that of the elastic peak.

The angular dependence of the surface-plasmon peak has been established by Stern and Ferrell[19] for the case of transmission through thin films. They found for the differential probability for the excitation of surface waves

$$\mu = \frac{dp}{d\Omega} = \frac{e^2}{\pi\hbar v}\,\frac{2}{1+\epsilon}\,\frac{\theta_E\theta}{(\theta_E^2+\theta^2)^2} f, \tag{1}$$

where $\theta = \hbar k/p$ is the scattering angle,

$$\theta_E = \frac{\hbar\omega s}{2E_0} = \frac{\hbar\Delta k}{p}$$

(E_0, primary energy; p and v, electron momentum and velocity), and f is a correction factor for a non-normal incidence:

$$f(\theta,\psi) = \left[\frac{1+(\theta_E/\theta)^2}{\cos^2\alpha} - \left(\cos\psi + \frac{\theta_E}{\theta}\right)^2\right]^{1/2}, \tag{2}$$

with α the angle of incidence and ψ an azimuth angle measured relative to the plane of incidence (here $\psi = 0$). For $\psi = 0$, f reduces to the value $f = (1 - \theta_E/\theta)$.

Thus for non-normally incident electrons the zero in the energy loss no longer coincides with the incident direction (as it is the case for normal incidence), but corresponds now with the scattering angle which makes the factor $f = 0$, i.e., for $\theta = \theta_E$.

This value of θ corresponds to a transfer momentum normal to the surface and thus there will be no excitation of surface waves. On the other hand the intensity of the inelastically scattered electrons appeared not to be symmetrical relative to the incident-beam direction.

But is it possible to extend the result of Stern and Ferrell to the case of a reflection experiment? We can assume a two-step process in which it would be possible to consider separately the two events: first the elastic scattering by the lattice and second the inelastic scattering by plasmon creation. Thus the scattering angle θ in formula (2) will be the angle between the specular direction and the reflected beam. The angular dependence given by formula (2) reduces in the case $\psi = 0$ to

$$g(\theta) = \frac{\theta\theta_E}{\theta^2+\theta_E^2}\left(1 - \frac{\theta_E}{\theta}\right). \tag{3}$$

Thus the zero in the energy loss corresponds to a direction which makes the angle $\theta_0 = \theta_E$ with the specular direction. For an incidence angle $\alpha = 60°$ and for 60-eV electrons, we find

$$\theta_0 \simeq 8.2°.$$

Now the maximum of $g(\theta)$ is obtained for two values of θ:

$$\theta_{m1} = 11.7°, \quad \theta_{m2} = -0.7°.$$

The greatest value for the loss maximum being obtained for the negative value of θ_m.

It is interesting to observe that the angular dependence given by formula (3) is identical with that obtained for reflection experiments by Lucas and Sunjic[20] and by Newns and Muscat[21] using a semiclassical approximation. In our angular experiment, however, we have to modify formula (3) in order to take into account the fact that the incidence angle α is no longer constant. Owing to the constancy of the scattering angle in our apparatus, a target rotation of angle γ will bring a beam at the entrance of the analyzer slit that makes the angle 2γ with the direction of the specular beam. Thus the preceding values are slightly altered. However, the experimental position of the maximum of the 9.5-eV peak versus the rotation angle does not agree very well with the theoretical result: the displacement from the specular direction is too large. We can only record that the asymmetrical effect shown in Fig. 5 is qualitatively consistent with the behavior of a surface plasmon.

2. *Interband transitions*

Certain other structures given in Table I may be attributed to interband transitions, but generally the interpretation of energy-loss spectra is very difficult especially for slow electrons. For faster electrons (10^3–10^5 eV) the dielectric theory of solids explains fairly well the inelastic scattering (Ref. 4, Bauer, and Ref. 15) and thus one can make a good comparison with optical data. Some discrepancies appear which are due to the major difference between optical and energy-loss-spectroscopy (ELS) methods: when the optical absorption is proportional to ϵ_2, the electron energy losses are proportional to $-\mathrm{Im}(1/\epsilon) = \epsilon_2/(\epsilon_1^2+\epsilon_2^2)$. Nevertheless, in practice we can identify, for sufficiently fast electrons, the dielectric constant due to the longitudinal field of electrons with the dielectric constant due to the transverse electromagnetic wave.[22] Thus energy losses can be used as optical data to give information on the three-dimensional band structure.

A theory of inelastic scattering of slow electrons ($\leq$100 eV) in solids was developed by Bauer[4] and showed that nondirect transitions were very probable in this case. With slow electrons solid-state

excitations have no negligible momenta ($K \neq 0$) compared to the dimensions of the reciprocal lattice and it is necessary to take into account the diffraction effects and the exchange forces. Thus we have to be very careful in comparing optical data, which mainly give the energy of direct interband transitions ($K=0$), with the energy losses of slow electrons, where the nondirect interband transitions ($K \neq 0$) are predominant.

However some rough comparisons can be made and structures appearing at the same energy position in both measurements may be identified as due to interband transitions.

2.4-, 4.2-, and 7.0-eV losses. For instance the peaks at 2.4, 4.2, and 7.0 eV agree with the peaks found for ϵ_2 in optical studies[18,23]: 1.8, 3.8, and 7.4 eV. Thus they may be attributed to bulk transitions.

Photoemission measurements on Mo films[23] show that there are three different initial-state structures in the energy distribution at 0.5, 1.6, and 3.9 eV below the Fermi level.

These results are consistent with another measurement of the optical density of states (including optical-transition probability factor) found for[24] Mo and giving structures at 0.5, 1.6, and 3.6 eV below the Fermi level. Recent photoemission measurements on the (100) and (110) faces of Mo give similar results[25]; optical density of states shows the following major features on the (100) face: 0.5, 1.8, 3.0, and 4.0 eV below the Fermi level.

Assuming a nondirect transition model for which the optical excitations are proportional to the product of the density of initial and final states, Kress and Lapeyre[23] calculate the optical density of final states. They find two structures at $\simeq 2$ and 3.8 eV above the Fermi level. All these experimental values are in fairly good agreement with the theoretical density of states,[26,27] which gives for initial states the values 1.5, 2.8, and 4.2 eV below the Fermi level and for the final state, 2 eV above the Fermi level. These results are summarized in the Fig. 6, where we have represented by horizontal solid lines the energy positions of the main structures given for the initial states, and by dashed lines the vacant states above the Fermi level. Figure 6(a) shows the results of Kress and Lapeyre.[23] We have represented by vertical dashed arrows a tentative interpretation of our transitions of energy 1.8, 3.8, and 7.4 eV. Figure 6(b) shows the results of theoretical calculations of the density of states by Matheiss[26] and Petroff and Viswanathan.[27] Thus some of the features we have found by ELS may be identified as bulk indirect transitions by comparison with optical and photoemission data.

4.2- and 5.1-eV losses. Nevertheless the attribution of the 4.2-eV loss to a bulk transition is not satisfactory for two reasons: first this transition is very intense on the clean surface, and, second, it disappears rapidly when impurities are allowed to adsorb. The same behavior is found for the 5.1-eV loss and we are led to assume that these losses are due to transitions involving a surface state as initial state (we can call them surface transitions).

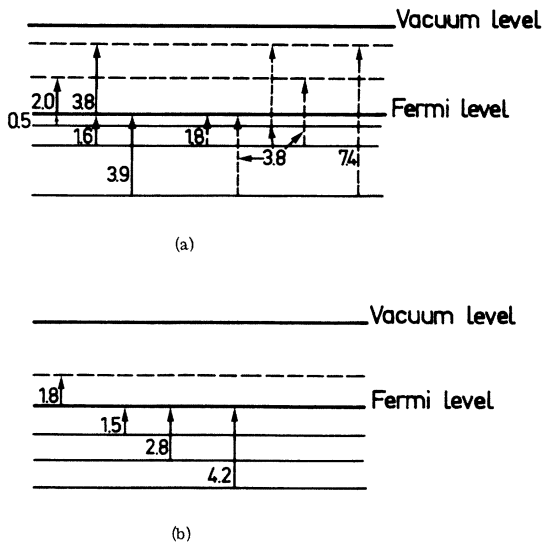

FIG. 6. (a) Solid arrows: transitions and energy levels found in Ref. 23; dashed arrows: possible transitions seen in the present work. (b) Peaks in the theoretical density of states (Refs. 26 and 27).

Recently the existence of a peak in the density of states 0.4 eV below the Fermi level has been demonstrated by field-emission and photoemission measurements[28,29] for the (100) face of tungsten. This structure has been attributed to a surface state that may exist in the gap owing to the spin-orbit splitting along the [100] direction (the ΓH direction in k space).[30,31] As molybdenum is nearly indentical to tungsten we can thus expect a similar behavior. In fact, earlier experiments of field emission on a molybdenum emitter[32] have shown an anomalous emission coming from a level situated 0.15 eV below the Fermi level (0.35 eV for W). This location is consistent with band-structure calculations for tungsten including spin-orbit interactions.[26] The application of a modified spin-orbit interaction parameter to the case of molybdenum gives a theoretical value for the band gap of 0.01 Ry $\simeq$ 0.14 eV. Thus we can expect, as in the case of W(100), a surface state close to the Fermi level for Mo(100). More recent calculations[33] based on the tight-binding approximation and using the moment method have shown evidence of surface states

on nondense planes of a transition metal. These surface states are not due in that case to spin-orbit coupling. The recent results of photoemission measurements on[25] Mo(100) seem also to corroborate the hypothesis of the surface state. Thus the measured transitions at 4.2 and 5.1 eV may be due to transitions coming from a surface state situated just below the Fermi level and terminating at different final states close to the vacuum level (the work function for the 100 face of molybdenum is $\simeq$4.8 eV).

These two transitions disappeared after an exposure to oxygen of 0.5 langmuir (1L = 10^{-6} Torr sec), but the 4.2-eV peak seems to be more sensitive to the oxygen exposure than the 5.1-eV peak. A shift of the 4.2-eV peak is also observed during the adsorption: its position varied from 4.2 to 3.6 eV for the 0.3-L exposition.

On the other hand the 5.1-eV peak is more sensitive to hydrogen adsorption: its maximum amplitude is divided by 2 for a hydrogen exposure of 0.4 L when the 4.2-eV peak is only slightly altered.

The loss at 1.25 eV may be due to a transition with the final state an empty state right above the Fermi level. The enhancement of this peak in the grazing-incidence case can suggest the possibility of a transition involving an empty surface state. However this structure seems too insensitive to contamination to maintain this assumption.

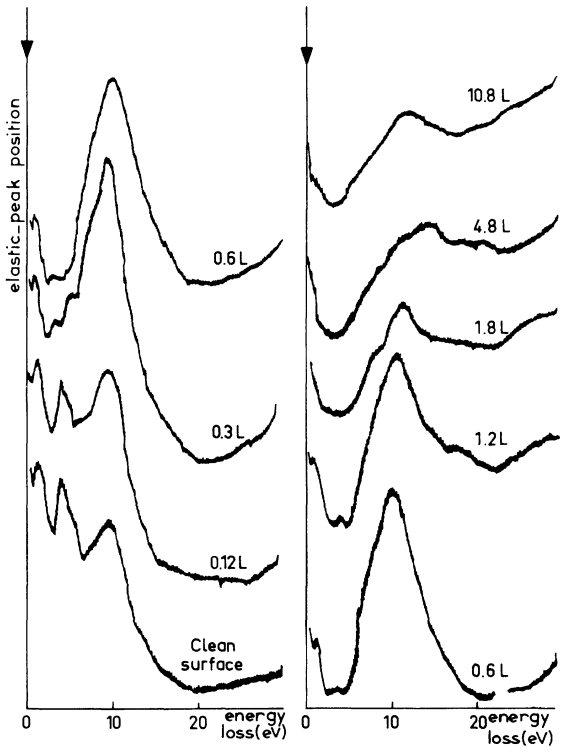

FIG. 7. Variations of the energy-loss spectrum during an oxygen adsorption. Primary energy, 60 eV.

D. Effects of oxygen adsorption

Figure 7 shows the overall variations of the energy-loss spectrum when the clean target is subjected to oxygen adsorption (E_p = 60 eV). The exposures to oxygen are given in langmuir and the energy-loss range is reduced to 20 eV. We can see the drastic modifications of the spectrum during adsorption: the two peaks centered near the 4.5-eV loss decrease in the early stage of adsorption; for the 0.6-L exposure they have completely disappeared. The huge surface-plasmon loss (near 10 eV) increases in height and in width, the last effect being mainly due to the growth of a new loss centered at about 7 eV, which appears as a shoulder on the 10-eV-loss peak for 0.3-L exposure; its position and height will be evidenced by the curve analysis. Above 1.8 L, the plasmon peak is strongly altered and is mixed with other losses. Another rough observation can be made: the background contribution increases as the adsorption goes on. The effect is appreciable from an exposure of 0.6 L and increases with further exposure. This modification extends from a secondary-emission region to an energy loss of 20 eV for 0.6-L exposure and begins to alter the loss region near the elastic peak for higher exposure.

1. Detailed analysis

Figures 8(a)–8(d) show the spectra obtained respectively for the clean surface and after exposures of 0.12, 0.3 and 0.6 L.

For the sake of clarity, the curve analysis has not been added to the last three curves; the locations given for the different peaks are the maxima of the Lorentzian profiles used to fit the experimental data. New peaks appear during the oxygen adsorption 2.4 and 4.3 eV, and a broad peak centered at 7.0 eV for an exposure of 0.6 L. A loss centered at 5 eV begins to grow for 1-L exposure. Small but broad peaks at 13.7, 18.2, and 21 eV appear for 0.6-L exposure. The 13.7-eV peak is shifted for higher exposures: it stabilizes at 15.4 eV for 1.8 L. The plasmon peak is continuously shifted from the clean value, 9.5 eV, to 10.3 eV for an exposure of 0.6 L. It continues to shift at a smaller rate for higher exposures. For exposures greater than 5 L the two main losses at 5 and 7 eV are always present but broaden and shift towards lower values. Above 10 L the different losses merge and the background contribution strongly increases on the low-energy region.

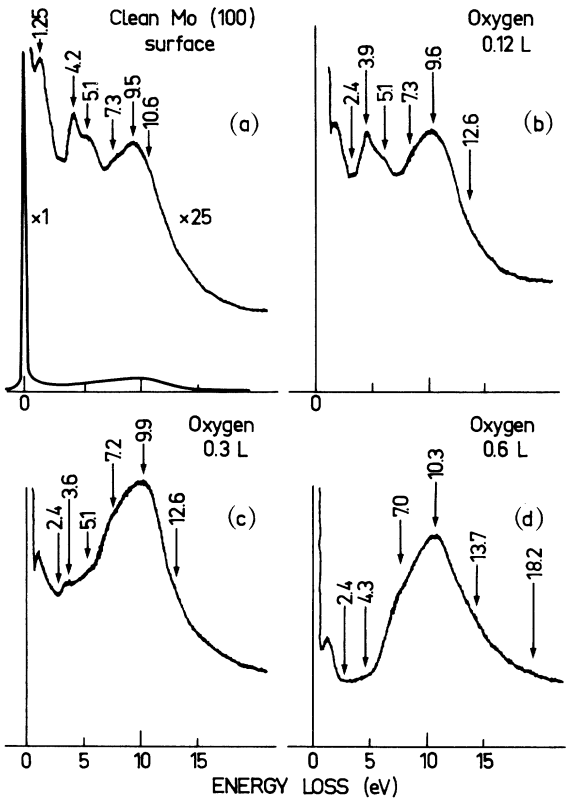

FIG. 8. Detailed analysis of energy-distribution curves obtained for different exposures to oxygen (E_p = 60 eV); arrows show the position of the main structures deduced from the curve analysis.

2. *Comparison with adsorption kinetics of oxygen on Mo(100)*

First we will summarize the main results obtained during a study of oxygen adsorption on a (100) molybdenum surface[34] with the techniques of LEED, Auger spectroscopy, and work-function measurements. There are some other studies of this adsorption and they are listed in Ref. 34. Useful comparison can be also made with oxygen adsorption on W(100), which has been widely studied.

Three main stages can be seen in the adsorption of oxygen on Mo(100):

(i) For exposure between 0 and 1 L. The LEED pattern consists of a C (2×2) structure which reaches its maximum intensity for 1 L. In this interval the relative oxygen coverage measured by the intensity of the oxygen Auger peak appeared to grow linearly with the exposure. The work function decreases and presents a minimum value corresponding to a change of 200 meV for about 1-L exposure.

(ii) 1–4 L. Facets appear and the C (2×2) structure has completely disappeared for an exposure of 3.5 L. The work function increases, reaches the clean-surface value for an exposure slightly smaller than 2 L, and begins to stabilize, for the 4-L exposure (for this exposure its increase is about 700 meV). The oxygen density increases at a smaller rate than in the first stage: the population for an exposure of 4 L is twice the population for 1 L.

(iii) Above 4 L. A P (3×1) structure is formed at the early stage and slowly disappears for further exposures. It is replaced at saturation by a P (1×1) or slightly amorphous structure. The work function begins to increase again to attain a value corresponding to a total $\Delta\phi$ of 1.8 eV at the saturation obtained for an exposure of about 12 L. The oxygen density increases at a smaller rate than in the preceding stage and for the saturation the population is thrice the population for 1 L.

Figure 9 shows the work-function changes measured in the present apparatus. We can thus, in comparing the curves of $\Delta\phi$ given in the two experiments, have a good check on our exposure scale. This is an important factor as we know the difficulties in measuring small oxygen pressures in an ultrahigh-vacuum system.[35]

The initial decrease of the work function is well reproducible under different pressure conditions, thus indicating that this decrease is not due to a possible CO formation in wall exchange or in the hot-cathode gauge. On the other hand CO adsorption on Mo(100) produces a decrease of work function smaller than 100 meV,[36] and the adsorption of residual gases (mainly H_2) produces an increase of the work function. No decrease of the work function was observed upon oxygen adsorption on W(100) at room temperature. This difference of behavior of the two metals has already been observed[37] and may be attributed in part to the difference of their cohesive energy.[34] There is some evidence that oxygen is adsorbed dissociatively in the early stages of adsorption.[38,34] Thus we have been led to assume that during these stages, oxygen atoms penetrate the lattice, thus explaining the initial decrease of work function. Such behavior

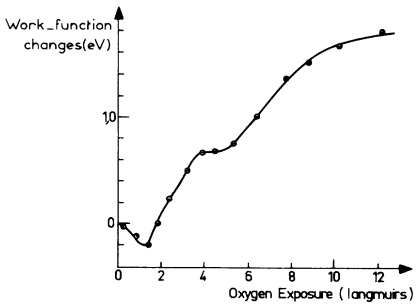

FIG. 9. Work-function change of the (100) Mo face versus the oxygen exposure.

may be compared with the adsorption of oxygen at high temperature (1000 K) on W(100),[39] which led to a decrease of the work function without loss of oxygen. The authors interpreted this fact by the penetration of oxygen atoms into the surface. In the case of Mo(100) we may conclude that this penetration occurs at room temperature and that the C (2×2) structure observed in the early stages of adsorption is a reconstructed one.

General information may be extracted from the loss spectra we have obtained during oxygen adsorption; this came from the modification of the elastic peak intensity, modification of the intensity and position of the surface-plasmon peak, and the appearance of new peaks.

Elastic peak intensity. Figure 10 shows the variation of the elastic peak intensity during the first stages of adsorption (solid curve).

There may be several reasons for the intensity modification of a diffracted beam, particularly the (00) beam[40]: modification of the primary beam intensity, structural changes, inelastic processes affecting the elastic yield, and the atomic scattering factor of the adsorbate.

The first factor has not to be taken into account owing to the good stability of the primary current. Inelastic processes would decrease the elastic intensity when the latter increases in the first stage of adsorption. The atomic scattering factor of oxygen may be higher than that of molybdenum in the particular direction we analyze with the present apparatus. But this interpretation is not consistent with our assumption of the penetration of oxygen atoms into the lattice. The only explanation we can retain is the structural change during the first stage of oxygen adsorption. The formation of the reconstructed C (2×2) structure may produce an enhancement of the elastic intensity in the analyzed direction (the plane of incidence contains the 11 direction in the crystal surface). The subsequent decrease of the elastic peak intensity is correlated with the appearance of microfacets on the surface.

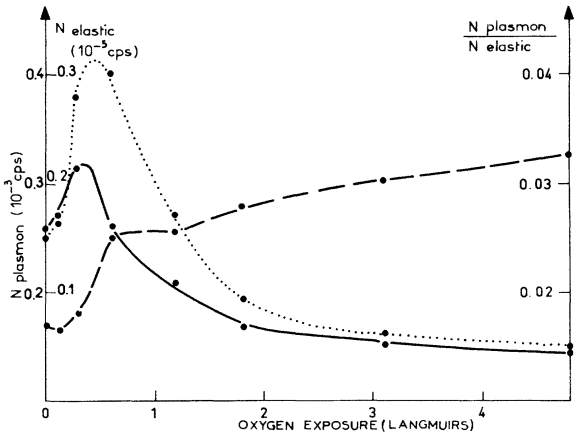

FIG. 10. Variation versus oxygen exposure of: solid curve, elastic peak amplitude; dotted curve, plasmon peak amplitude; dashed curve, plasmon–to–elastic-peak ratio. (N_{elastic} : number of electrons on the elastic peak; N_{plasmon}: number of electrons on the plasmon peak.)

Modifications on surface-plasmon peak. The $\simeq$10-eV energy loss we have identified as the surface plasmon shows a behavior similar to the elastic peak; its intensity seems to have a maximum value near the 0.5-L exposure (dotted curve on Fig. 10). We have represented the plasmon-peak–to–elastic-peak ratio (dashed curve), the intensity of plasmon peak being given by the curve analysis. It appears to increase up to 0.5 L, then stabilizes and increases again for exposures greater than 1 L.

Thus the plasmon peak relative to the elastic peak seems to increase during adsorption. However we must bear in mind the inaccuracy we have for the measured intensity of the loss peak in such experiments. Of greater interest and less subject to imprecision is the energy-loss value associated with the surface-plasma oscillation. Figure 11 shows the shift of the surface-plasmon peak during the adsorption. There is a rapid increase of energy loss, the value 10.5 eV being obtained for about 1 L; then there is a plateau and the loss increases again from 1.2 to 4 L, where a maximum value of 11.3 eV is obtained.

The initial shift of the surface plasmon is correlated with the formation of the C (2×2) structure, i.e., the penetration of oxygen atoms into the surface layer.

For greater exposures the plasmon peak is again shifted and it seems changed in shape and width from 1.6- to 1.8-L exposures, suggesting thus a modified energy loss. This modified energy loss may be due to an oxide formation on the surface,

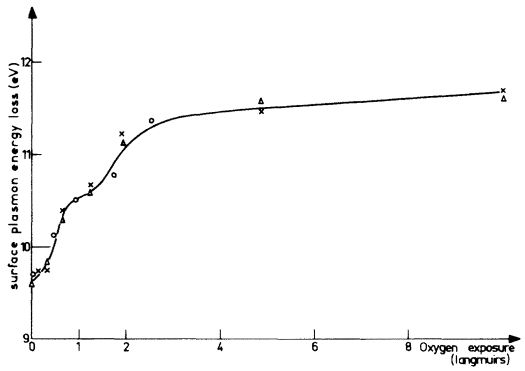

FIG. 11. Surface-plasmon energy loss versus oxygen exposure.

thus leading to a new value of the surface plasmon.

An alternative explanation of the 10-eV-peak shift may be found in the recent interpretation given by Weaver, Lynch, and Olson[41] for this energy loss. They deduced from optical measurements that Mo (as Ta and V) exhibits two volume and two surface plasmons. This interpretation has been already given by Zashkvara and Red'kin[42] to explain the results they obtained in an experiment of reflection of 1-keV electrons on a molybdenum surface: they observed a shift of both surface- and volume-plasmon peaks when the scattering angle of the electrons was varied. For the authors the peaks due to surface excitation are enhanced relative to the peaks due to volume excitation as the scattering angle decreases, explaining thus the shifts observed. Thus, in our case the 10-eV peak would be formed by a surface plasmon at 9.5 eV which disappeared during oxygen adsorption and by a volume plasmon at 10 eV or more which is enhanced relative to the elastic peak by the disappearance of the surface plasmon. Such an explanation seems to hold good for vanadium[43]; nevertheless in our experiment on molybdenum we were unable to separate, in the 10 eV peak, two different losses. In a future apparatus, the possibility of moving the analyzer and target will allow us to study the angular dependence of both surface and volume plasmons and thus answer the question.

Peaks due to the adsorbate. New peaks appear during the adsorption of oxygen. They are probably due to transitions involving the energy level of adsorbed oxygen. These transitions may be due to the excitation of electrons from molecular orbitals formed during the chemisorption to an empty state. But there are several possibilities for this empty state: it may be a vacant level of the metal or an excited state of the chemisorbed molecule.[44] On the other hand, the method of ELS gives only the energy difference between these two states and we have to make assumptions about their respective positions. The comparison with photoemission data when available will give us the position of the possible initial state relative to the Fermi level of the metal and then the results of ELS will allow us to determine the position of the final state. Thus this position is given relative to the Fermi level of the metal but we can say nothing about its nature: it can be a vacant level of the metal or an excited state of the "surface complex."

The major feature in the spectrum obtained during oxygen adsorption on Mo(100) is a loss peak centered at 7.2 eV which in the early stage of adsorption is mixed with the clean-surface transition at 7.3 eV. For higher exposure this peak is slightly displaced towards lower-energy loss values (7.2 to 6.9 eV) and its FWHM appears to be about 2.2 eV. It may be due to a transition involving the $2p$ level of oxygen. Photoemission measurements on Mo(100),[25] and W(110) and W(100),[1] have shown the formation during oxygen adsorption of a virtual level centered roughly about 6 eV below the Fermi level. Thus the energy loss at 7.2 eV we have measured is probably due to a transition between a virtual level of oxygen at 6 eV below the Fermi level and an empty state situated near the Fermi level.

The 7-eV loss appears at the beginning of the adsorption thus in the frame of our tentative model it can be correlated with the presence in the first layers of molybdenum of oxygen atoms strongly bound to the metal atoms. Figure 12 represents the spectra obtained on an oxygen-covered surface (about 5 L) for different primary energies: 20 to 60 eV. We can see that the position of the 6.9-eV peak is unchanged and only its amplitude relative to the 11-eV peak amplitude is increased as the incident energy decreases. For a primary energy of 20 eV, only the 6.9-eV peak is still important. Two main results appear: first the location of the 6.9-eV loss is independent of the primary energy thus eliminating some spurious effects (diffraction, etc.), and second, it is possible by the choice of the energy to discriminate between different losses and to make sure, for instance, of the existence of very small structures in a too-rich spectrum.

The 5-eV loss growing from the 1-L exposure may be attributed to oxygen adsorbed on the (110)

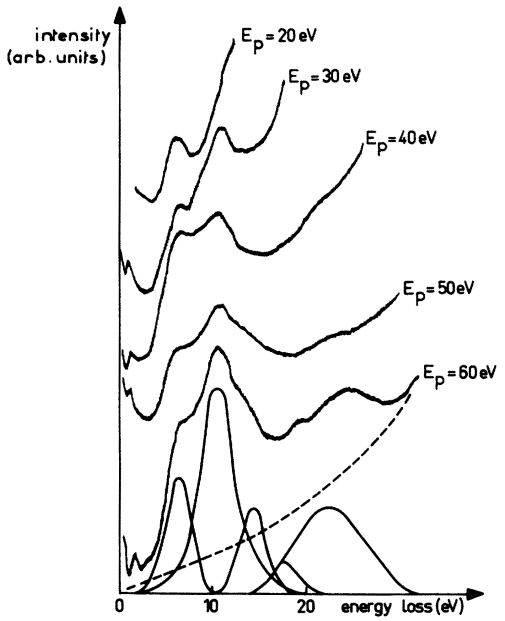

FIG. 12. Energy-distribution curves for an oxygen-covered Mo(100) surface for different primary energies.

microfacets formed at this stage.[34] For comparison we have shown in Fig. 13 a spectrum obtained with the oxidized surface after 3 h in 10^{-6} Torr of oxygen at a temperature of 1000°C. This spectrum is only qualitatively different from the spectrum obtained with the surface covered by oxygen adsorbed at room temperature in the exposure range 2 to 3 L. The peak at 7 eV is slightly displaced: it appears now at 6.8 eV but its intensity is greatly enhanced and comparable to the 10-eV peak; its FWHM of 3.3 eV is appreciably increased. The 5-eV loss is also present as in the case of adsorption at room temperature.

Thus in the present state of our technique it is difficult to unambiguously discriminate between chemisorbed oxygen atoms and oxygen bound to molybdenum atoms in an oxide state. This result may be compared to that obtained in an ESCA (electron spectroscopy for chemical analysis study of the oxygen adsorption on polycrystalline tungsten,[45] where it appears that there is no important change in the shape or position of the O(1s) line between adsorbed oxygen and oxide phases formed on the surface.

We have also, in such a study, to be very well aware of the possible effects of the primary electron beam on the chemisorbed layer. At the energies used in these measurements many modifications can be caused by the incident electrons: electron-stimulated desorption, conversion between the different adsorbed phases, etc. We can roughly evaluate the effect of electronic desorption in our experiment. The area of the target

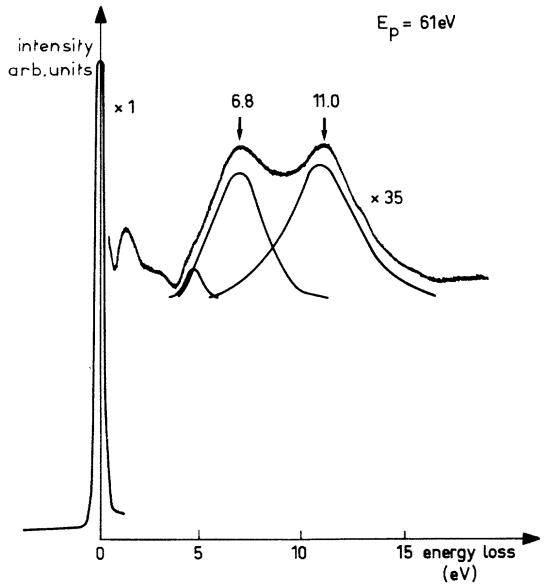

FIG. 13. Energy-distribution curve for an oxidized surface; 3 h in 10^{-6} Torr of oxygen at 1000°C.

submitted to the electron beam is about 1 mm^2, the current delivered by the monochromator being in the range 10^{-10} A, say 10^{-8} A/cm^2. There are no published data of the cross section for electron desorption of oxygen on Mo(100), but we can take the value given by Madey[46] for W(100). On W(100) there are two states of adsorbed oxygen according to their behavior upon electron impact: the β_2 state formed at the beginning of the oxygen adsorption, which is relatively "electronically inactive," and the β_1 phase growing from about 3-L exposure, which has an important cross section for electronic desorption. If we take for the total cross section for electronic desorption of the β_1 phase a mean value $Q \simeq 10^{-19}$ cm^2,[46] we find a total yield of oxygen atoms and ions desorbed $I = 3.1 \times 10^6$ atoms/cm^2 sec $= 1.5 \times 10^6$ desorbed oxygen molecules per cm^2 sec for an oxygen coverage of 5×10^{14} molecules/cm^2. Thus during a typical time required to obtain a spectrum with a good signal-to-noise ratio, i.e., about 10 min (5 scans of 2 min each), about 10^9 oxygen molecules are desorbed on 1 cm^2 of molybdenum initially covered by 5×10^{14} oxygen molecules.

This yield is relatively small but not negligible and we must carefully try to decrease this effect, the only way being at the present time to increase the luminosity of the analyzer, allowing us to decrease the density of the incident electron beam.

IV. CONCLUSION

Energy-loss spectroscopy of slow electrons appears to be a very sensitive method for studying gas adsorption on metal surfaces. Surface effects may be emphasized by the reflection technique and by the choice of the primary energy; using a suitable analysis method, much useful information can be obtained on the electronic structure of the metal surface and adsorbed species.

The spectra are often complex and difficult to interpret, especially in terms of the band structure of the solid. They are complicated by the occurrence with great probability of indirect interband transitions. However, in the case of chemisorption studies it is not necessary to know very well the electronic structure of the clean metal as we proceed by the difference between the two states: clean surface and surface with determined amount of adsorbed gases. On the other hand, comparison between energy-loss spectroscopy, photoemission, and reflectance measurements[47] will be very useful for understanding the electronic properties of solid surfaces. It will give information on the initial states of the transitions as well as on the emply final states. The advantage of ELS over optical measurements is that its surface sensi-

tivity permits us to see transitions to empty surface states. We have seen, in comparing the results of the present study with photoemission results on similar systems, that the value measured for the transition is very close to the energy of adsorbed-atom levels measured from the Fermi level in photoemission experiments. Thus we can suppose that, at least for Mo(100), the empty final states of the measured transitions are flat and very close to the Fermi level.

Energy-loss spectroscopy can also be used to determine the cleanliness of the surface. When the reproducible spectra of the clean surface are well known, very small quantities of adsorbed species can be determined by the changes they produce. The sensitivity depends upon the studied system but is probably in the range 0.01 monolayer. Thus a chemisorption kinetic can be accurately followed in keeping in mind the possible effect of the electron beam on the surface compounds. This method, as do other spectroscopic methods, needs comparison with more classical techniques for surface study such as LEED, work-function, and flash-desorption measurements. Owing to the difficulty in achieving all these measurements in the same apparatus it is necessary to dispose of a common technique on the different experimental vessels which enables the working conditions to be controlled.

Finally the ELS performed with a movable analyzer will give more interesting information on the surface- and volume-plasmon behavior and probably on the symmetry of the adsorbed molecules.

ACKNOWLEDGMENTS

We should like to thank Dr. D. M. Newns for many helpful discussions and communication of unpublished results he obtained with Dr. J. P. Muscat. We also wish to thank Dr. Baptiste of the C. I. S. I. for performing the programming of the analysis method.

[1]J. M. Baker and D. E. Eastman, J. Vac. Sci. Technol. 10, 223 (1973); B. J. Waclawski and E. W. Plummer, J. Vac. Sci. Technol. 10, 292 (1973); B. Feuerbacher and B. Fitton, Phys. Rev. B 8, 4890 (1973).
[2]J. W. Gadzuk and E. W. Plummer, Rev. Mod. Phys. 45, 487 (1973).
[3]H. D. Hagstrum and G. E. Becker, J. Chem. Phys. 54, 1015 (1971).
[4]E. Bauer, Z. Phys. 224, 19 (1969); F. Steinrisser and E. N. Sickafus, Phys. Rev. Lett. 27, 992 (1971); J. Kuppers, Surf. Sci. 36, 53 (1973); S. Ohtani, K. Terada, and Y. Murata, Phys. Rev. Lett. 32, 415 (1974).
[5]R. Riwan, C. Guillot, and J. Lecante, C. R. Acad. Sci. B 274, 502 (1972).
[6]L. A. Harris, Surf. Sci. 15, 77 (1969).
[7]P. Marmet and L. Kervin, Can. J. Phys. 38, 787 (1960).
[8]Y. Ballu, Rev. Phys. Appl. 3, 46 (1968).
[9]L. N. Tharp and E. J. Scheibner, J. Appl. Phys. 38, 3320 (1967).
[10]A. Bagchi and C. B. Duke, Phys. Rev. B 5, 2784 (1972).
[11]P. J. Estrup and J. Anderson, Surf. Sci. 8, 101 (1967).
[12]P. S. P. Wei, J. Chem. Phys. 53, 2939 (1970).
[13]J. C. Tracy, in *Electron Emission Spectroscopy*, edited by W. Dekeyser, L. Fiermans, G. Vanderkelen, and J. Vennik (D. Reidel, Dordrecht, Holland, 1973), p. 295.
[14]M. J. Lynch and J. B. Swan, Aust. J. Phys. 21, 811 (1968).
[15]C. Guillot, J. Lecante, and R. Riwan, Vide 164, 79 (1973).
[16]H. Raether, Springer Tracts Mod. Phys. 38, 84 (1965).
[17]R. H. Ritchie, Phys. Rev. 106, 874 (1957).
[18]D. W. Juenker, L. J. Le Blanc, and C. R. Martin, J. Opt. Soc. Am. 58, 164 (1968).
[19]E. A. Stern, and R. A. Ferrell, Phys. Rev. 120, 130 (1960).
[20]A. A. Lucas, and M. Sunjic, Progress in Surface Science 2, pt. 2, p. 75 (unpublished).
[21]D. M. Newns and J. P. Muscat, unpublished results (private communication).
[22]H. Raether, Helv. Phys. Acta 41, 1112 (1968).
[23]K. A. Kress and G. J. Lapeyre, in *Third Materials Research Symposium, Gaithersburg, Maryland, 1969*, Natl. Bur. Stand. (U.S.) Publ. 323 (U.S. GPO, Washington, D. C., 1969).
[24]D. E. Eastman, Solid State Commun. 7, 1697 (1969).
[25]R. Cinti and Al Khoury (private communication).
[26]L. F. Mattheiss, Phys. Rev. A 139, 1893 (1965).
[27]L. Petroff and C. R. Viswanathan, Phys. Rev. B 4, 799 (1971).
[28]B. J. Waclawski and E. W. Plummer, Phys. Rev. Lett. 29, 783 (1972).
[29]B. Feuerbacher and B. Fitton, Phys. Rev. Lett. 29, 786 (1972).
[30]F. Forstman and V. Heine, Phys. Rev. Lett. 24, 1419 (1970).
[31]J. W. Gadzuk, J. Vac. Sci. Technol. 9, 591 (1971).
[32]L. W. Swanson, and L. C. Crouser, Phys. Rev. Lett. 19, 1179 (1967).
[33]M. C. Desjonqueres and F. Cyrot-Lackmann, J. Phys. (Paris) 36, 245 (1975); J. Phys. F 5, 1368 (1975).
[34]R. Riwan, C. Guillot, and J. Paigne, Surf. Sci. 47, 183 (1975).
[35]J. McNobbs, Vacuum 23, 391 (1973).
[36]J. Lecante, R. Riwan, and C. Guillot, Surf. Sci. 35, 271 (1973).
[37]J. T. Yates, Jr. and T. E. Madey (private communication).
[38]N. P. Vas'ko, Yu G. Ptushinskii, and B. A. Chuikov, Surf. Sci. 14, 448 (1969).
[39]Ya. P. Zingerman and V. A. Ishchuk, Sov. Phys.-Solid State 8, 2394 (1967); P. J. Estrup, in *Structure and Chemistry of Solid Surfaces*, edited, by G. A. Somorjai (Wiley, New York, 1969), p. 19-1.
[40]Y. Margoninski, Surf. Sci. 29, 355 (1972).
[41]J. H. Weaver, D. W. Lynch, and C. G. Olson, Phys.

Rev. B 10, 501 (1974).
[42]V. V. Zashkvara and V. S. Red'kin, Sov. Phys.-Solid State 14, 2410 (1973).
[43]G. W. Simmons and E. J. Scheibner, J. Appl. Phys. 43, 693 (1972).
[44]T. B. Grimley, *Molecular Processes on Solid Surfaces*, edited by E. Drauglis, R. D. Gretz, and R. I. Jaffee (McGraw-Hill, New York, 1969), p. 299.
[45]J. T. Yates, Jr., T. E. Madey, and N. E. Erickson, Surf. Sci. 43, 257 (1974).
[46]T. E. Madey, Surf. Sci. 33, 355 (1972).
[47]G. W. Rubloff, J. Anderson, and P. J. Stiles, Surf. Sci. 37, 75 (1973).